Pick-up Calibration in CESR Beam Position Monitors

Beau Meredith
Department of Physics, Greenville College, Greenville, IL, 62246
(Dated: August 21, 2003)

The beam position algorithm presently used in the Cornell Electron Storage Ring (CESR) does not accurately resolve the position of the beam at large displacements from the beam pipe center. To reduce this problem, a new beam position algorithm is being implemented. This paper discusses the implementation of this new algorithm, and also additional corrections made for misalignments of the beam position monitor buttons.

I. INTRODUCTION

Identifying the position of electron and positron bunches is a very important task for accelerator physics inside the Cornell Electron Storage Ring (CESR). Accurate positioning simplifies accelerator and luminosity tuning and enables simple testing of the magnetic elements inside the ring. The beam position monitors (BPM's) inside CESR consist of four button pick-ups, or electrodes, which measure a signal due to a charged bunch (Fig. 1).

The current method used to resolve the position assumes that combinations of the four signals s_i are proportional to the transverse beam position (x, y) and is termed the *difference over sum* method [1]. The transverse position is calculated using the following equations:

$$x = x_0 \frac{(s_2 + s_4) - (s_1 + s_3)}{\sum_i s_i}, \tag{1}$$

$$y = y_0 \frac{(s_3 + s_4) - (s_1 + s_2)}{\sum_i s_i}, \tag{2}$$

where x_0 and y_0 are scale factors.

The *difference over sum* method for converting BPM signals to position works well for beams near the center of the beam pipe, but the linear relationship breaks down at large displacements. The pretzel orbit in CESR has large displacements and thus renders the *difference over sum* method ineffective. The implementation of a method that accurately

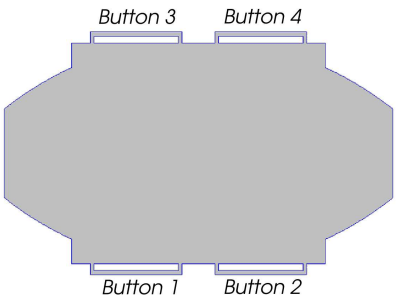

FIG. 1: 2D transverse cross section of a CESR arc BPM. The white rectangles represent the buttons and the gray area is the interior of the vacuum pipe.

resolves beam positions at large displacements from the beam pipe center is described in this paper. For this, a new beam position algorithm based upon a 2D electrostatic model of the BPM's was developed. Furthermore, calibration coefficients were introduced that account for geometrical misalignment of BPM buttons. The two processes will first be briefly described, followed by a description of their implementation and measurements that test their usefulness.

II. 2D ELECTROSTATIC MODEL

Using the 2D electrostatic model, a general method for finding the beam position has been developed that can be used for beams at an arbitrary transverse position in the beam pipe, whereas the linear *difference over sum* method is only accurate for small transverse displacements. The conditions necessary for accuracy of the 2D method are ultra-relativistic speeds and sufficiently long beam bunches. When these conditions are met, the 3D problem of converting measured signals from the 3D BPM structure to transverse positions simplifies into a 2D electrostatic problem [2]. This 2D problem consists of finding the position (x, y) of a stationary charge given the four measured button signals, s_1, s_2, s_3, s_4. One could compute potentials at the button pick-ups directly for a large set of beam positions (x,y). However, this would involve many electrostatic calculations and would be very time consuming. Instead, a useful and efficient solution is used that only requires one electrostatic calculation [3]. A description of this solution method follows.

Consider the two separate cases inside a beam position monitor (Fig. 2):

1. A static charge at position (x,y) inside the BPM with all electrodes grounded,
2. Placing a potential on button i with no charge inside the BPM and buttons j, $j \neq i$ grounded.

A relationship given by Green's Reciprocity theorem [3] is $q_{si} = \frac{q}{V_b}\phi_i(x, y)$, where q_{si} is the induced charge on button i in case 1, q is the charge at (x, y) in case 1, $\phi_i(x, y)$ is the potential at (x, y) in case 2, and V_b is the voltage on button i in case 2. The measured signals are assumed to be proportional to the induced charge, and so $s_i = kq_{si} = \frac{kq}{V_b}\phi_i(x, y)$, where k is a constant of proportionality. Using this relationship for $i = 1, 2, 3, 4$ with V_b constant, the position of the beam can be found by

1. Calculating ϕ_i for a large set of positions inside the interior of a BPM.
2. Minimizing the following χ^2 of the fit between normalized signals and normalized potentials,

$$\chi^2 = \sum_i \left(\frac{s_i}{\sum_j s_j} - \frac{\phi_i(x, y)}{\sum_j \phi_j(x, y)}\right)^2. \tag{3}$$

The charge q, button voltage V_b, and proportionality constant k are all eliminated by dividing each s_i by $\sum_j s_j$, leaving only a dependence on $\phi_i(x, y)$. Thus, the division of signal s_i by the sum of signals and the division of the potential $\phi_i(x, y)$ by the sum of potentials should yield two normalized quantities that are equal, or

$$\frac{s_i}{\sum_j s_j} = \frac{\phi_i(x, y)}{\sum_j \phi_j(x, y)}. \tag{4}$$

These four constraints ($i = 1, 2, 3, 4$) are used in the χ^2 minimization to find the two transverse position parameters x and y. The problem is over-constrained, but this should not affect the solution unless there are faulty signals.

The minimization is performed by an algorithm that systematically searches different transverse positions, which correspond to different potentials $\phi_i(x, y)$, and finds the position where the χ^2 is smallest.

The electrostatic field solver *Poisson* was used to solve for the potentials inside the BPM's. This was done for each type of BPM used in CESR including the Arcs, and those at quadrupole magnets Q0, Q1, Q2, Q48, and Q49. An output file was created for each BPM type and contains a table of potentials, $\phi_1(x, y)$, calculated at an evenly spaced grid of points. All the BPM's contain geometrical symmetries that allow each $\phi_i(x, y)$, $i = 2, 3, 4$, to be calculated by a simple rotation or reflection of coordinates in the table. The grid spacing for each output file is approximately 0.12 cm. To obtain potentials at positions between grid points, the algorithm uses a bicubic spline interpolation.

III. BUTTON MISALIGNMENT

The previous method is a general one, but it assumes that the buttons are perfectly aligned. That is, they are aligned exactly as specifications dictate. In reality, there are small differences between the actual and specified positions of the electrodes. Consider an increase in the height of a button relative to the surface of the vacuum chamber. Because of the increased distance of the button pick-up to a beam, the value of the measured button signal due to a beam will decrease. This change in button signal causes a small error in the calculated position of the beam. Corrections for this type of error utilize a set of calibration

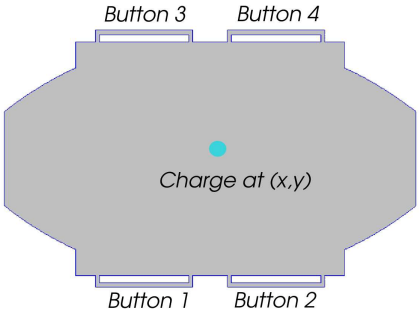

(a) Physical representation of case 1

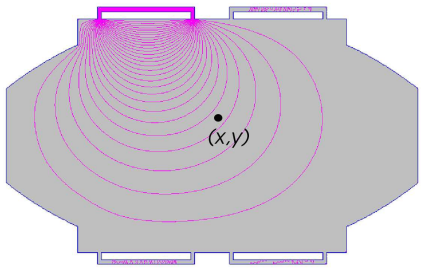

(b) Physical representation of case 2 for $i = 3$ and $V_b = 10V$. V_b is placed on button 3 and all the other buttons are grounded. The potential is calculated throughout the interior of the BPM by Poisson Electric Field Solver.

FIG. 2: Two different electrostatic problems related by Green's Reciprocity Theorem.

coefficients that are unique to each BPM. A complete derivation of these coefficients can be found in Keil [4].

If a beam passes through a BPM with misaligned button i, then the measured potential on button i will be $\tilde{U}_i = b_i U_i$, where U_i is the potential that would be induced on a perfectly aligned button, and b_i is the calibration coefficient associated with button i. The measured signal s_i is assumed to be proportional to the measured potential $\tilde{U}_i = b_i U_i$, and thus s_i contains information about the button misalignment. The χ^2 minimization, Eqn. 3, assumes perfect alignment of the buttons, and so each s_i must be divided by b_i to create the signals of perfectly aligned buttons. These "perfect" signals are then put into the minimization algorithm in order to resolve the beam position. Thus, the importance of the calibration coefficients is that they improve upon the beam position accuracy of the algorithm.

To find the value of the each calibration coefficient, a spectrum analyzer was used to place a known RF signal on one button and measure the RF signal on another button. The buttons are separated by space and so the measurement is analogous to placing a potential on one plate of a capacitor and measuring the potential on the other plate, with each "plate" being connected to ground by a termination resistor. The measurement is related to the capacitive coupling of the two buttons, and so it contains information about the misalignment and calibration coefficients of both. Let $\tilde{U}_{ij}$ be the measured RF signal on button j due to placing a RF signal on button i, and let U_{ij} be the RF signal on button j due to an RF signal on button i if all the buttons were perfectly aligned. The relationship between the measured signal and perfect button signal is $\tilde{U}_{ij} = b_i b_j U_{ij}$ [4]. To find b_1, b_2, b_3, and b_4, six measurements must be made, $\tilde{U}_{12}$, $\tilde{U}_{13}$, $\tilde{U}_{14}$, $\tilde{U}_{24}$, $\tilde{U}_{23}$, $\tilde{U}_{43}$, that encompass all measurement combinations. Then the following two relationships of a BPM with perfectly aligned buttons are utilized:

1. The coupling between i and j is the same as between j and i, and hence $\tilde{U}_{ij} = \tilde{U}_{ji}$ assuming the terminating resistances are all equal (they are designed to be).

2. Physical symmetries dictate that $U_{12} = U_{43}$, $U_{13} = U_{24}$, $U_{14} = U_{23}$ (again, assuming that the termination resistances are equal). This comes from the fact that the button configurations are symmetric about the BPM's horizontal and vertical axes.

Each b_i is solved for in terms of b_1. The χ^2 minimization process uses ratios of the b_i, so they can be scaled arbitrarily. Setting $b_1 = 1$ and solving for b_2, b_3, and b_4 yields the following equations for the calibration coefficients:

$$b_1 = 1 \tag{5}$$

$$b_2 = \sqrt{\frac{\tilde{U}_{23}\tilde{U}_{24}}{\tilde{U}_{13}\tilde{U}_{14}}} \tag{6}$$

$$b_3 = \sqrt{\frac{\tilde{U}_{23}\tilde{U}_{43}}{\tilde{U}_{12}\tilde{U}_{14}}} \tag{7}$$

$$b_4 = \sqrt{\frac{\tilde{U}_{24}\tilde{U}_{43}}{\tilde{U}_{12}\tilde{U}_{13}}} \tag{8}$$

The signal measured by the spectrum analyzer is the signal across the termination resistor of button j with resistance R, and hence $\tilde{U}_{ij} = V_R$. A simple RC series circuit has the

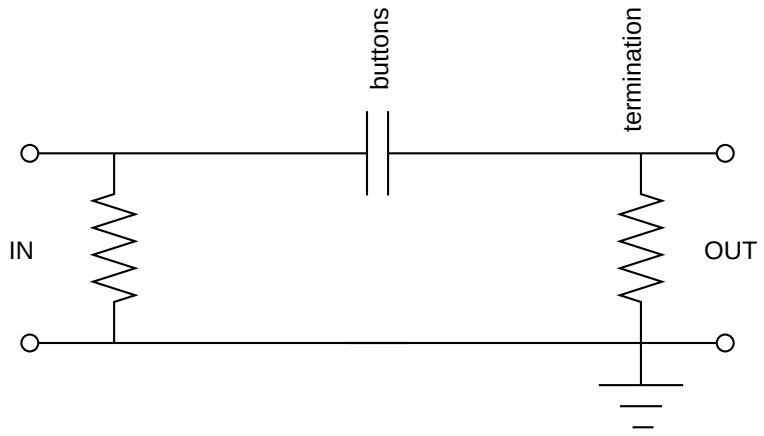

FIG. 3: Beam position monitor circuit diagram.

relationship that $V_R = \frac{V_{max} RC\omega}{\sqrt{1+(RC\omega)^2}}$. When $\omega << \frac{1}{RC}$, then the linear relationship between potential and frequency, $V_R = V_{max} RC\omega$, holds. Assuming a parallel plate capacitor model of the buttons, $\frac{1}{RC}$ is near 100 GHz. The real capacitance is much smaller than that of the parallel plate model, and hence $\frac{1}{RC} > 100$ GHz. Since the maximum ω used is 100 MHz << 100 GHz $< \frac{1}{RC}$, the spectrum analyzer measurements should produce an output signal that is linearly proportional to ω. Each $\tilde{U}_{ij}$ is linearly proportional to ω, and so the quotients in the Eqns. 5 through 8 cancel out the dependence of b_i on ω (Note: this only applies when the signal is linearly proportional to ω). Hence, only the slope of the RF signal vs. ω curve needs to be known to calculate the coefficients. Actual measurements consist of measuring the slopes of a $\tilde{U}_{ij}$ vs. ω curve. These slopes are then put into Eqns. 5 through 8 to calculate the calibration coefficients.

IV. PROCEDURE

The calibration coefficients for each BPM in the CESR ring were measured using an HP3588 Spectrum Analyzer. The buttons not involved in a particular measurement were grounded with shorting caps. Each measurement was made by putting a known RF signal on one button and measuring the slope of the resulting RF signal on another button with a frequency sweep of 1 to 100 MHz (Fig. 4). The circuit diagram for the BPM simplifies to a simple series RC circuit (Fig. 3), and so a fairly linear signal response curve was expected and observed. The rationale for using the 1-100 MHz span was that the measurements stopped being linear outside these bounds. Possible causes of nonlinearity include standing waves inside the coax cables, cable interference, and outside noise. Each measurement consisted of averaging 70 individual measurements using the exponential averaging feature available on the spectrum analyzer.

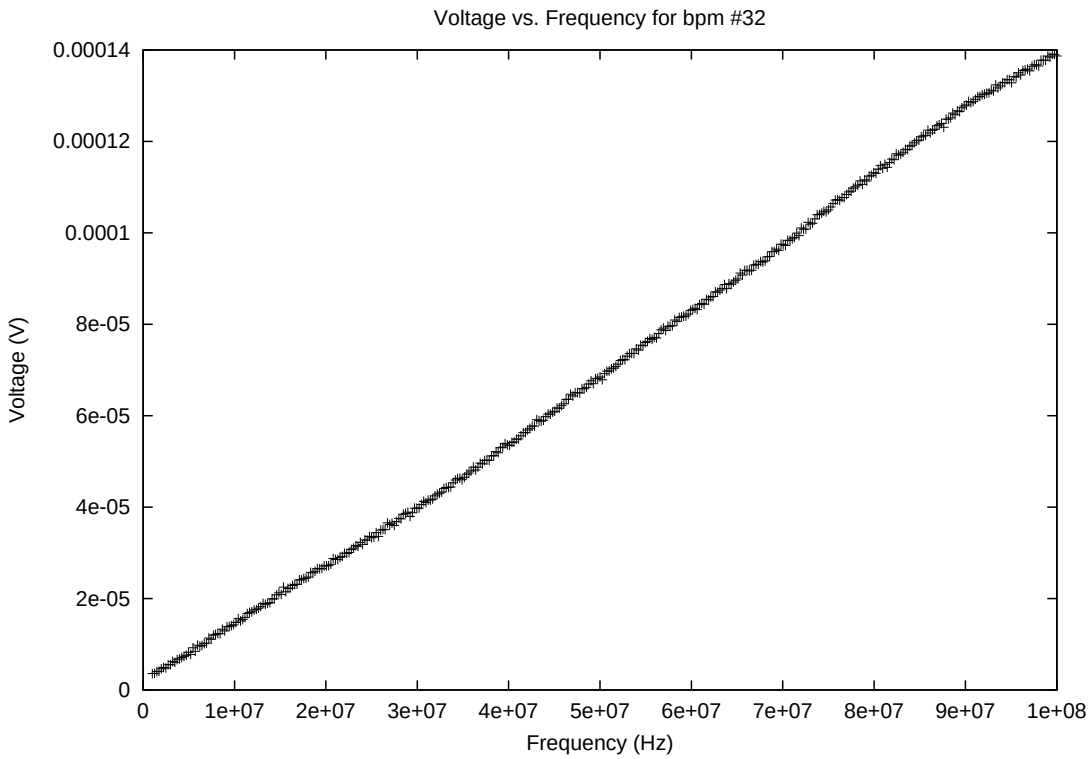

FIG. 4: Sample spectrum analyzer measurement.

V. PROCEDURAL NOTES

Because of the symmetry argument made in the *Button Misalignment* section, only six measurements were performed. However, this assumed that all terminating resistances were identical for a particular BPM. In reality, they are not identical and can vary by up to 1Ω out of 80Ω. This affects the theoretical argument in two ways:

1. Reversing the source and output buttons will change the measurement. If $R_i \neq R_j$, then
$$\tilde{U}_{ij} = V_{max} R_j C\omega \neq V_{max} R_i C\omega = \tilde{U}_{ji}. \tag{9}$$
Hence the assumption $\tilde{U}_{ij} = \tilde{U}_{ji}$ is no longer valid.

2. If only six measurements are taken, all the values of the termination resistors must be known to correctly calculate each b_i.

The termination resistances were obtained by recording the value written on each BPM and were used in the calculation of each b_i. However, they did not significantly improve the fitting, and so their usefulness is questionable. For this reason, any reference to implementation of calibration coefficients in the proceeding sections does not use the termination resistors.

VI. RESULTS OF CALIBRATION

The values of the calibration coefficients usually ranged from 0.93 to 1.07. For most BPM's, the χ^2 of the fit was smaller when the coefficients were used as compared to when

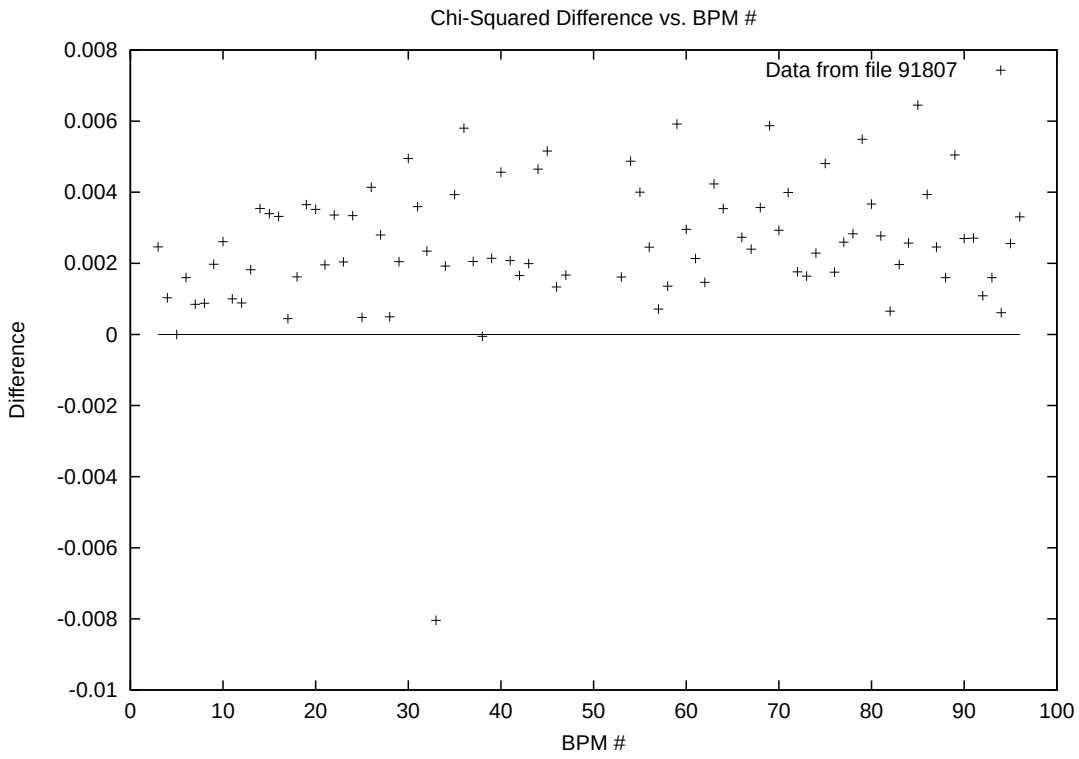

FIG. 5: Plot of difference in χ^2 when the coefficients are not used and when they are. The BPM number, which identifies its position in the ring, is on abscissa. The measurements were taken during one complete orbit of a beam bunch in the ring.

they were not used (Fig. 5). A smaller χ^2 of the fit indicates better accuracy of beam position, which in turn leads to the conclusion that the coefficients make an improvement to the beam positioning system. However, there were BPM's where the χ^2 of the fit did not improve when the coefficients were used. Calibration measurements were repeated for two of these BPM's. The new calibration data did not improve the χ^2, and so it can be reasonably concluded that the signals from these BPM's are corrupted in some other way.

VII. TESTING

Two tests were performed with the new beam positioning algorithm:

1. Vary pretzel amplitude and measure horizontal position,
2. Vary horizontal and vertical separator voltages by fixed increments and measure the position.

The relationship between horizontal beam position and pretzel amplitude is basically linear. Fig. 6 shows that the old beam position algorithm, or *difference over sum* method, became nonlinear at displacements of about 1 cm, whereas the new algorithm, or 2D electrostatic method, keeps its linear relationship out to the highest displacement shown. This linear relationship shows that the new algorithm is behaving as one would predict when varying the pretzel amplitude, and shows that it is much more accurate at large displacements from the beam pipe center.

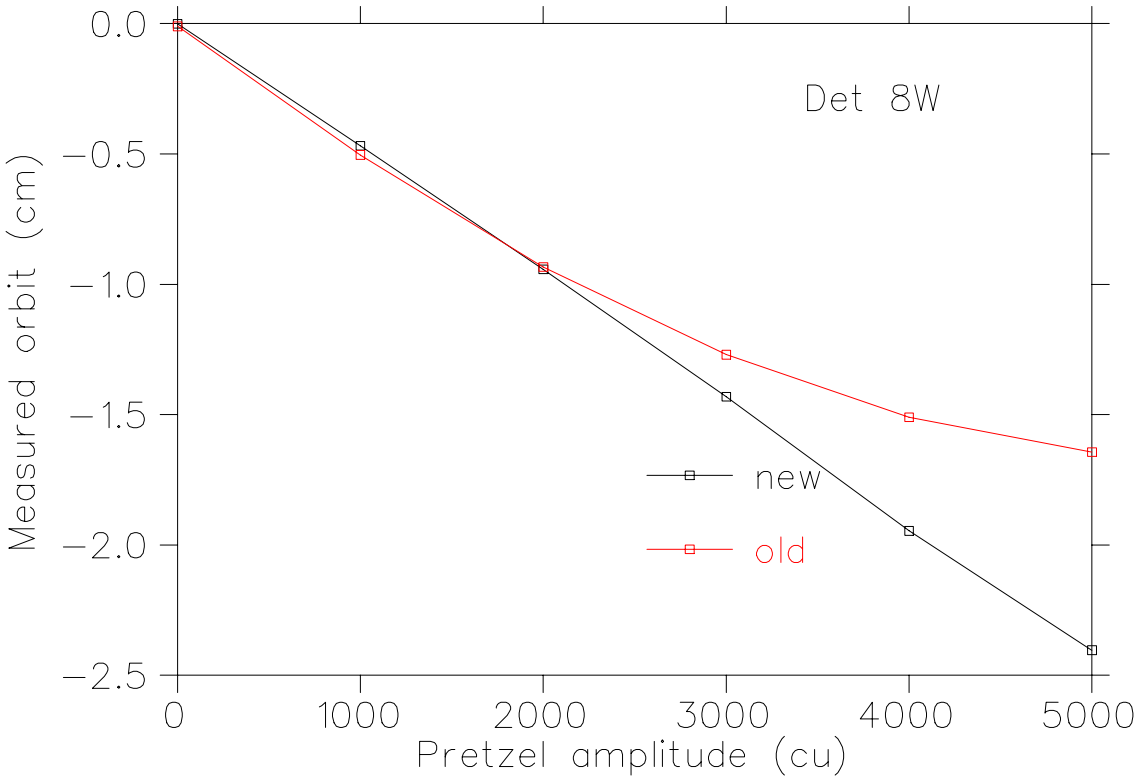

FIG. 6: Horizontal Position vs. Pretzel Amplitude

Varying the horizontal and vertical separator voltages by fixed increments and calculating the resulting positions should yield a very uniform looking grid. This is because changes in separator voltages are linearly proportional to changes in position. Fig. 7 shows the *difference over sum* calculated positions in red and the 2D electrostatic calculated positions in black. At large displacements from the beam pipe center, the edges in the plot for the *difference over sum* method begin to curve and show a nonlinear relationship between position and separator voltage. The 2D electrostatic method keeps a fairly linear relationship at the outer edges. This is further evidence that the new algorithm being implemented does in fact improve position resolution for large displacements.

VIII. CONCLUSIONS & RECOMMENDATIONS

Preliminary testing of the new beam position monitor algorithm used by CESR shows that it is more accurate than the old algorithm in resolving the position of the beam at large displacements from the beam pipe center. In addition, the inclusion of the calibration coefficients seems to improve the positioning accuracy of the BPM's. It is recommended to use the calibration coefficients on the BPM's where the χ^2 of the fit improves.

IX. ACKNOWLEDGMENTS

I would like to to thank the NSF and Professor Richard Galik of Cornell University for providing me this wonderful opportunity to do research. Also, I would like to thank graduate

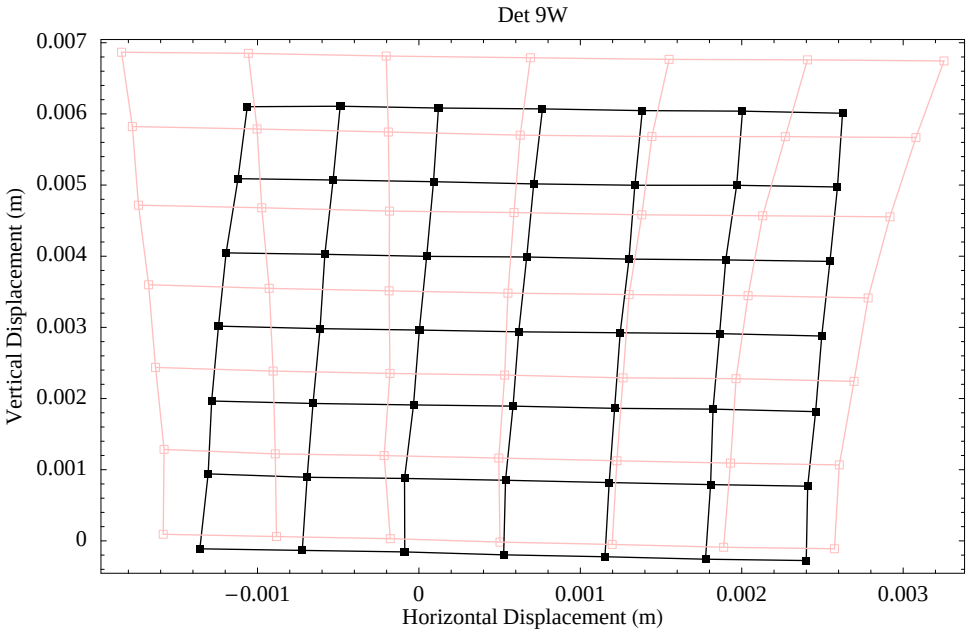

FIG. 7: Calculated positions of varying separator by fixed increments

student Rich Helms and Professor Georg Hoffstaetter of Cornell University, who proposed this REU project and guided me through the experience. In addition, special thanks go to J. Sikora, R. Meller, J. Urban, Y. Li, J. Smith, M. Palmer, C. Strohman, and J. Kandaswamy for helping me at various points in my project.

This work was supported by NSF REU grant PHY-0101649 and the research cooperative agreement PHY-9809799.

---

[1] P. Bagley and G. Rouse, Laboratory of Nuclear Studies, Cornell University, CBN 91-17 (1991).
[2] J. H. Cuperus, Nuclear Instruments and Methods **220**, (1977) 145.
[3] R. Helms *et al.*, Laboratory for Elementary Particle Physics, Cornell University, CBN 03-15 (2003).
[4] J. Keil, Ph.D. thesis, Bonn University, 2000.